2.14 Hyperon Resonance Studies from Charm Baryon Decays at BaBar

Veronique Ziegler
Thomas Jefferson National Accelerator Facility
Newport News, VA 23606, U.S.A.

Abstract

We present studies of hyperon and hyperon resonance production in charm baryon decays at BaBar. The helicity formalism employed to measure the spin of Ω^- was extended to three-body final states whereby the properties of the $\Xi(1690)^0$ and $\Xi(1690)^0$ produced in Λ_c^+ decay where obtained.

1. Introduction

The data samples used for the analyses described in this note were collected with the BaBar detector at the PEP-II asymmetric-energy e^+e^- collider. In these studies, the charm baryons are inclusively produced in e^+e^- collisions at center-of-mass energies 10.58 and 10.54 GeV. The BaBar detector and reconstruction software are described elsewhere [1].

2. General Procedure for Charm Baryon Selection

The selection of charm baryon candidates requires the sequential reconstruction of initial and intermediate state candidates using four-momentum addition of tracks. Particle identification selectors based on specific energy loss ($\mathrm{d}E/\mathrm{d}x$) and Cherenkov angle measurements have been used to identify proton, pion and kaon final tracks. Each intermediate state candidate is required to have its invariant mass within $\pm 3\sigma$ of the fitted peak position of the relevant distribution, where σ is the mass resolution. In all cases, the fitted peak mass is consistent with the expected value, and the intermediate state invariant mass is then constrained to this value. Due to the fact that each weakly-decaying intermediate state (*i.e.*, the K_S and hyperons) is long-lived, the signal-to-background ratio is improved by imposing a vertex displacement criterion (in the direction of the momentum vector). In order to further enhance signal-to-background ratio, a selection criterion is imposed on the center-of-mass momentum p^* of the parent charm baryon. The use of charge conjugate states is implied throughout in this note.

3. Formalism

Measurements of the Ω^- spin are obtained using a primary sample obtained from the decay sequence $\Xi_c^0 \to \Omega^- K^+$, with $\Omega^- \to \Lambda K^-$ [2]. It is assumed that each charm baryon type has spin 1/2 and, as a result of its inclusive production, that it is described by a diagonal spin projection density matrix. The analysis does not require that the diagonal matrix elements be equal.

By choosing the quantization axis along the direction of the Ω^- in the charm baryon rest-frame, the Ω^- inherits the spin projection of the charm baryon [2]. It follows that, regardless of the spin J of the Ω^-, the density matrix describing the Ω^- sample is diagonal, with non-zero values only for the $\pm 1/2$ spin projection elements, *i.e.*, the helicity λ_i of the Ω^- can take

only the values $\pm 1/2$. Since the final state Λ and K^- have spin values 1/2 and 0, respectively, the net final state helicity λ_f also can take only the values $\pm 1/2$.

Defining the helicity angle θ_h as the angle between the direction of the Λ in the rest-frame of the Ω^- and the quantization axis, the probability for the Λ to be produced with Euler angles $(\phi, \theta_h, 0)$ with respect to the quantization axis is given by the square of the amplitude ψ, characterizing the decay of an Ω^- with spin J and helicity λ_i to a 2-body system with net helicity λ_f, where $\psi = A^J_{\lambda_f} D^{J\,*}_{\lambda_i \lambda_f}(\phi, \theta_h, 0)$, and the transition matrix element $A^J_{\lambda_f}$ represents the coupling of the Ω^- to the final state. The angular distribution of the Λ is then given by

$$I \propto \sum_{\lambda_i, \lambda_f} \rho_{ii} \left| A^J_{\lambda_f} D^{J\,*}_{\lambda_i \lambda_f}(\phi, \theta_h, 0) \right|^2 , \tag{1}$$

where the ρ_{ii} ($i = \pm 1/2$) are the diagonal density matrix elements inherited from the charm baryon, and the sum is over all initial and final helicity states.

The Λ angular distribution integrated over ϕ is then obtained for spin hypotheses $J_\Omega = 1/2$, $3/2$, and $5/2$, respectively as follows:

$$dN/d\cos\theta_h \propto 1 + \beta \cos\theta_h, \tag{2}$$

$$dN/d\cos\theta_h \propto 1 + 3\cos^2\theta_h + \beta \cos\theta_h (5 - 9\cos^2\theta_h), \tag{3}$$

$$dN/d\cos\theta_h \propto 1 - 2\cos^2\theta_h + 5\cos^4\theta_h + \beta \cos\theta_{\rm h} (5 - 26\cos^2\theta_h + 25\cos^4\theta_h), \tag{4}$$

where the coefficient of the asymmetric term, β [2], may be non-zero as a consequence of parity violation in charm baryon and Ω^- weak decay.

The angular distributions of the decay products of the Ω^- baryon resulting from a spin 1/2 charm baryon decay are well-described by a function $\propto 1 + 3\cos^2\theta_h$. These observations are consistent with spin assignments 3/2 for the Ω^-. Values of 1/2 and greater than 3/2 for the spin of the Ω^- yield C.L. values significantly less than 1% when spin 1/2 is assumed for the parent charm baryon.

(a) **The Use of Legendre Polynomial Moments in Spin Determination**

For spin J, the corrected angular distributions can be written

$$\frac{dN}{d\cos\theta_h} = N \left[\sum_{l=0}^{l_{max}} \langle P_l \rangle P_l \left(\cos\theta_h \right) \right] ,$$

where $P_l\left(\cos\theta_h\right)$ are normalized Legendre Polynomial functions such that $l_{max} = 2J - 1$, and if l is odd $\langle P_l \rangle = 0$. Each assumed J defines l_{max}, so that $\langle P_l \rangle = 0$ for $l > l_{max}$ and $\langle P_l \rangle$ is calculable. The number of Ω^- signal events in a given mass bin is obtained by giving each event, j, in that bin, a weight $w_j = \frac{P_{l_{max}}\left(\cos\theta_{h_j}\right)}{\langle P_{l_{max}} \rangle}$.

In particular, for $J = 3/2$, giving each event a weight $w_j = \sqrt{10} P_2(\cos\theta_{h_j})$ projects the complete Ω^- signal. In order to test the $J = 5/2$ hypothesis, each event is given a weight $w_j = \frac{7}{\sqrt{2}} P_4(\cos\theta_{h_j})$.

As expected, the $\sqrt{10}P_2(\cos\theta_h)$ moment projects out the signal of a spin 3/2 hyperon, whereas the $7/\sqrt{2}P_4(\cos\theta_h)$ moment does not. These moments are used in the analysis of the $\Xi(1690)$ and $\Xi(1530)$ resonances described in the next section.

4. **Study of Cascade Resonances Using Three-body Charm Baryon Decays**

Although considerable advances have been made in baryon spectroscopy over the past decade, there has been very little improvement in our knowledge of hyperon resonances since 1988. The $\Xi(1690)$ has been observed in the $\Lambda\bar{K}$, $\Sigma\bar{K}$ and $\Xi\pi$ final states with various degrees of certainty.

(a) **The $\Xi(1530)^0$ from $\Lambda_c^+ \to \Xi^-\pi^+K^+$ Decay**

The properties of the Xi(1530) resonance are investigated in the $\Lambda_c^+ \to \Xi^-\pi^+K^+$ decay process [3]. The Dalitz plot for $\Lambda_c^+ \to \Xi^-\pi^+K^+$ is dominated by the contribution from $\Lambda_c^+ \to \Xi(1530)^0K^+$, where $\Xi(1530)^0 \to \Xi^-\pi^+$ by strong decay. The Dalitz plot (Fig. 1) shows evidence for only one resonant structure. A clear band can be seen at the nominal mass squared of the $\Xi(1530)^0 \to \Xi^-\pi^+$. The analysis of the Legendre polynomial moments of the $\Xi(1530)^0 \to \Xi^-\pi^+$ system established quite clearly, on the basis of Figs. 2(b) and 2(c), that the $\Xi(1530)^0$ hyperon resonance has spin 3/2. In conjunction with previous analyses [4] this also definitively establishes positive parity. However, comparison of the $P_2(\cos\theta_\Xi)$ moment to the $\Xi^-\pi^+$ mass distribution and fits to the angular decay distribution in the $\Xi(1530)^0$ region indicate that it is necessary to include other $\Xi^-\pi^+$ amplitudes in order to obtain a complete description of the data. In particular, the observation of a $P_1(\cos\theta_\Xi)$ moment exhibiting oscillatory behavior in the $\Xi(1530)^0$ region indicates the need for an $S_{1/2}$ amplitude, while providing first evidence for the expected rapid BW phase motion of the $P_{3/2}$ $\Xi(1530)^0$ amplitude. However, a simple model incorporating only these amplitudes and a $D_{5/2}$ amplitude is ruled out because of the failure to describe the $\Xi(1530)^0$ line shape. The presence of the $S_{1/2}$ amplitude at high mass and the behavior of the mass distribution near 1.7 GeV/c^2 suggest that a resonant $\Xi(1690)^0$ amplitude may be adding coherently to this amplitude, thus leading to the inference of spin-parity $1/2^-$ for the $\Xi(1690)^0$. It appears that a quantitative description of the $\Xi(1530)^0$ line shape, and indeed of the entire Dalitz plot, must incorporate these features together with amplitude contributions associated with the $K^+\pi^+$ and/or the Ξ^-K^+ systems. However such an analysis requires a higher statistics data sample.

(b) **The $\Xi(1690)^0$ from $\Lambda_c^+ \to (\Lambda\bar{K}^0)K^+$ Decay**

The $\Xi(1690)^0$ is observed in the $\Lambda\bar{K}^0$ system produced in the decay $\Lambda_c^+ \to (\Lambda\bar{K}^0)K^+$, where the $\bar{K}^0$ is reconstructed via $K_S \to \pi^+\pi^-$.

The selection of Λ_c^+ candidates requires the intermediate reconstruction of oppositely-charged track pairs consistent with $\Lambda \to p\,\pi^-$ and $K_S \to \pi^+\,\pi^-$ decays. A clear peak, significant skewed toward high mass, is seen in the vicinity of the $\Xi(1690)^0$.

The second and fourth order Legendre polynomial moments as a function of the mass of the (ΛK_S) system display no peaking structure at the position of the $\Xi(1690)^0$, which suggests that the $\Xi(1690)^0$ spin is probably 1/2. However, the Λ helicity cosine ($\cos\theta_\Lambda$) distribution is not flat in contrast to the expectation for a spin 1/2 to 1/2 transition.

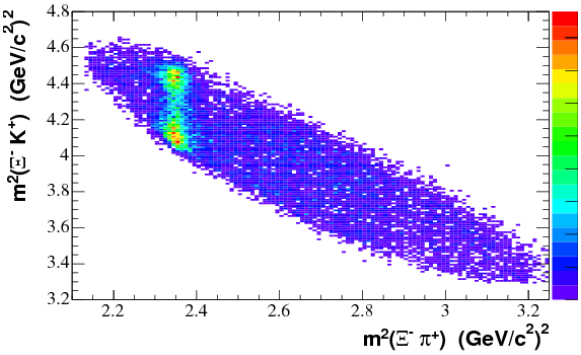

Figure 1: The Dalitz plot for $\Lambda_c^+ \to \Xi^-\pi^-K^+$ corresponding to the Λ_c^+ signal region.

The Dalitz plot of $\Lambda_c^+ \to \Lambda\bar{K}^0K^+$ signal candidates is shown, without efficiency-correction, in Fig. 3(a). A clear band is observed in the mass-squared region of the $\Xi(1690)^0$, together with an accumulation of events in the $\bar{K}^0K^+$ threshold region; the latter is consistent with a contribution to the Dalitz plot due to the $a_0(980)^+$ resonance. In contrast, the Dalitz plots corresponding to the Λ_c^+ mass-sideband regions exhibit no structure.

We describe the event distribution in the Dalitz plot of Fig. 3(b) in terms of an isobar model consisting of the coherent superposition of amplitudes characterizing $(\Lambda a_0(980)^+)$ and $(\Xi(1690)^0K^+)$ decay of the Λ_c^+. The $a_0(980)$ is known to couple to both $\eta\pi$ and $\bar{K}K$ and is characterized by the Flatté parametrization [5], while a Breit-Wigner function is used to describe the amplitude for the $\Xi(1690)^0$.

This model is used to describe the intensity distribution at a point on the Dalitz plot by means of the squared modulus of a coherent superposition of these two amplitudes, under the assumption that the $\Xi(1690)^0$ has spin 1/2, since the moment projections favor this choice. Fits to the Dalitz plot under the assumptions of spin 3/2 and 5/2 are ongoing. We find that no additional isobars are needed in order to accurately model the data. In order to extract the mass and width parameters of the $\Xi(1690)^0$, we perform a binned maximum Likelihood fit to the rectangular Dalitz plot of Fig. 3(b) (incorporating resolution smearing in mass, and a background parametrization obtained from the Λ_c^+ mass-sidebands).

The fit reproduces accurately the skewed lineshape of the ΛK_S invariant mass projection (Fig. 4). The skewing results from the interference between the $a_0(980)^+$ and the $\Xi(1690)^0$. The actual $\Xi(1690)^0$ signal is symmetric and significantly smaller than the apparent signal, which is dominated by this interference effect. The fit also provides an excellent representation of the other invariant mass projections.

5. Conclusions

Mass and width measurements for the $\Xi(1690)^0$ have been obtained from fits to the $\Lambda_c^+ \to \Lambda K_S K^+$ Dalitz plot. The results indicate that the spin of the $\Xi(1690)$ is consistent with 1/2. The properties of the $\Xi(1530)^0$ are studied using the decay $\Lambda_c^+ \to \Xi^-\pi^+K^+$. The spin of

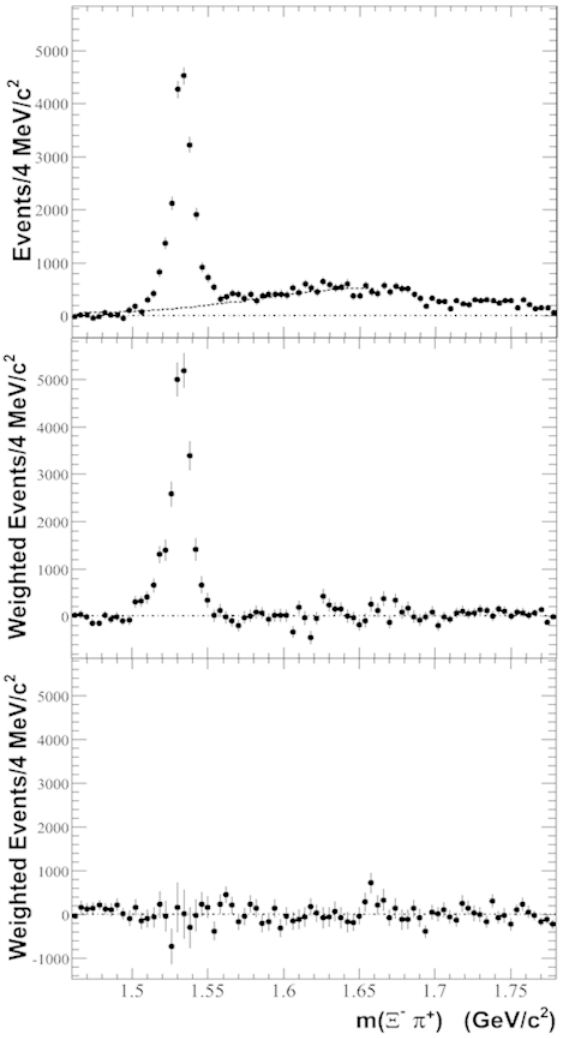

Figure 2: The efficiency-corrected $P0, 2, 4$ moments of the $\Xi^-\pi^+$ system invariant mass distribution for the Λ_c^+ signal region. In (a) the dashed curve represents the estimated background contribution in the Λ_c^+ region.

the $\Xi(1530)$ is consistent with 3/2.

Similar studies for cascade resonance production and associated spectra done at BaBar using charm baryon production can be done at GlueX with a K_L beam. Three-body systems involving two-body Cascade resonance decays require the analysis of the entire Dalitz plot when the statistical level is such that the shortcomings of a quasi-two-body approach become apparent. Therefore it is essential to have high statistics to allow for a proper to fit to the entire Dalitz plot.

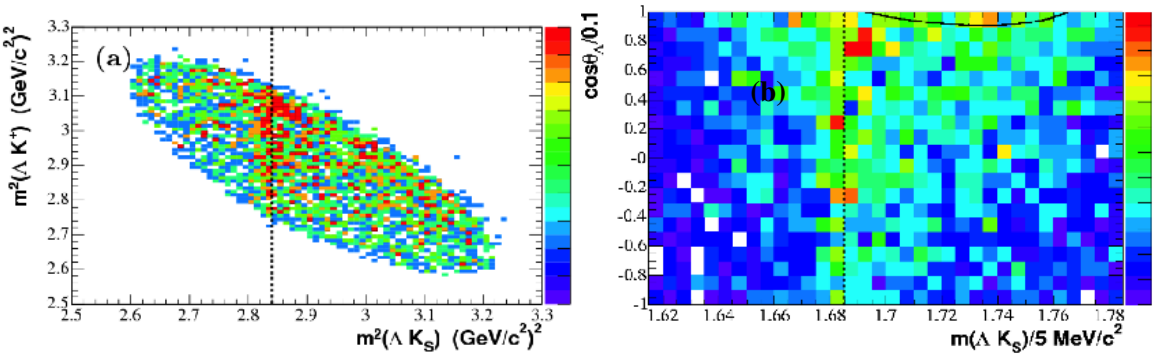

Figure 3: (a) The Dalitz plot for $\Lambda_c^+ \to \Lambda\bar{K}^0K^+$ corresponding to the Λ_c^+ signal region. The dashed line indicates the nominal mass-squared region of the $\Xi(1690)^0$. (b) The rectangular Dalitz plot for $\Lambda_c^+ \to \Lambda\bar{K}^0K^+$ corresponding to the Λ_c^+ signal region. The black curve corresponds to the $a_0(980)^+$ pole position.

Preliminary

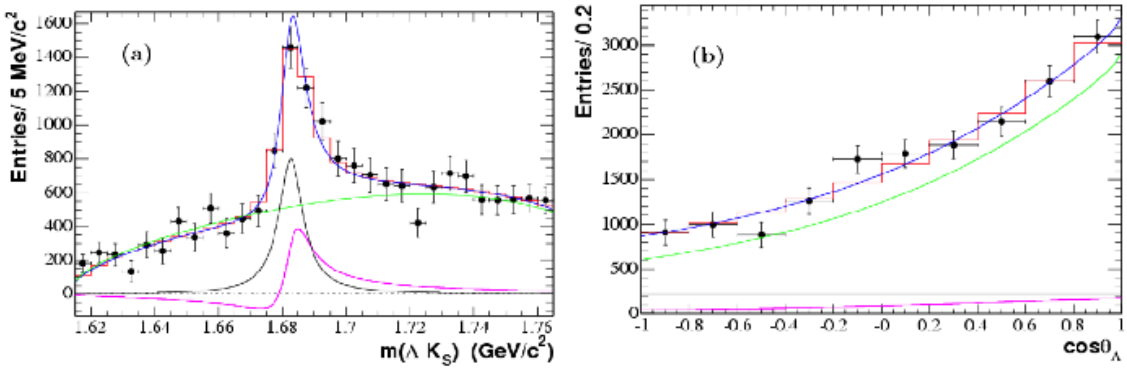

Figure 4: (a) Λ_c-mass-sideband-subtracted efficiency-corrected ΛK_S invariant mass projection. (b) Λ_c-mass-sideband-subtracted efficiency-corrected $\cos\theta_\Lambda$ spectrum.

6. **Acknowledgments**

This work was supported by DOE and NSF (USA), NSERC (Canada), IHEP (China), CEA and CNRS-IN2P3 (France), BMBF and DFG (Germany), INFN (Italy), FOM (The Netherlands), NFR (Norway), MIST (Russia), and PPARC (United Kingdom).

References

[1] B. Aubert *et al.*, Nucl. Instr. Meth. A **479**, 1 (2002).

[2] B. Aubert *et al.*, Phys. Rev. Lett. **97**, 112002 (2006).

[3] B. Aubert *et al.*, Phys. Rev. D **78**, 034008 (2008).

[4] P.E. Schlein *et al.*, Phys. Rev. Lett. **11**, 167 (1963); J. Button-Schafer *et al.*, Phys. Rev. **B142**, 883 (1966).

[5] S.M. Flatté, Phys. Lett. B **63**, 224 (1976).